Mouse Cytotoxic T Cell-derived Granzyme B Activates the Mitochondrial Cell Death Pathway in a Bim-dependent Fashion*

Elena Catalán[‡§1], Paula Jaime-Sánchez[‡§2], Nacho Aguiló[¶], Markus M. Simon[∥], Christopher J. Froelich[**], and Julián Pardo[‡§¶‡‡§§3]

From the ‡Departamento Bioquímica y Biología Molecular y Celular, §Biomedical Research Centre of Aragon, IIS Aragon, and ¶Departamento Microbiología, Medicina Preventiva y Salud Publica, Universidad de Zaragoza, 50009 Zaragoza, Spain, the ∥Metschnikoff Laboratory, Max-Planck-Institute for Immunology and Epigenetics, 79108 Freiburg, Germany, the **NorthShore University Health Systems Research Institute, University of Chicago, Evanston, Illinois 60201, the ‡‡Nanoscience Institute of Aragon, University of Zaragoza, 50015 Zaragoza, Spain, and the §§Aragon I+D Foundation, 50015 Zaragoza, Spain

Background: Cytotoxic T cells employ perforin and granzyme B to kill tumor cells.
Results: Bim-deficient 3T9-transformed MEF cells are resistant to gzmB-induced apoptosis.
Conclusion: The mitochondrial apoptotic pathway activated via Bim is critically involved in apoptosis induced by mouse granzyme B.
Significance: Learning how granzyme B induces apoptosis in different tumor cell types will help to predict and increase the efficacy of cancer immunotherapy.

Cytotoxic T cells (Tc) use perforin and granzyme B (gzmB) to kill virus-infected cells and cancer cells. Recent evidence suggests that human gzmB primarily induces apoptosis via the intrinsic mitochondrial pathway by either cleaving Bid or activating Bim leading to the activation of Bak/Bax and subsequent generation of active caspase-3. In contrast, mouse gzmB is thought to predominantly induce apoptosis by directly processing pro-caspase-3. However, in certain mouse cell types gzmB-mediated apoptosis mainly occurs via the mitochondrial pathway. To investigate whether Bim is involved under the latter conditions, we have now employed *ex vivo* virus-immune mouse Tc that selectively kill by using perforin and gzmB (gzmB+Tc) as effector cells and wild type as well as Bim- or Bak/Bax-deficient spontaneously (3T9) or virus-(SV40) transformed mouse embryonic fibroblast cells as targets. We show that gzmB+Tc-mediated apoptosis (phosphatidylserine translocation, mitochondrial depolarization, cytochrome *c* release, and caspase-3 activation) was severely reduced in 3T9 cells lacking either Bim or both Bak and Bax. This outcome was related to the ability of Tc cells to induce the degradation of Mcl-1 and Bcl-X_L, the anti-apoptotic counterparts of Bim. In contrast, gzmB+Tc-mediated apoptosis was not affected in SV40-transformed mouse embryonic fibroblast cells lacking Bak/Bax. The data provide evidence that Bim participates in mouse gzmB+Tc-mediated apoptosis of certain targets by activating the mitochondrial pathway and suggest that the mode of cell death depends on the target cell.

Our results suggest that the various molecular events leading to transformation and/or immortalization of cells have an impact on their relative resistance to the multiple gzmB+Tc-induced death pathways.

Cytotoxic T cells (Tc)[4] and natural killer cells control viral infections and cellular transformation, in part through the granule secretory pathway where the pore-forming protein perforin (perf) delivers a family of serine proteases, the granzymes, into the cytosol of the target cell (1–3). Tc cells are recognized as novel tools to eliminate cancer cells that do not respond to conventional treatments.

Among granzymes, gzmB is the most potent pro-apoptotic mediator in a variety of *in vitro* propagated target cells (3–6). The apoptotic potential of other granzymes such as gzmA and gzmK remains controversial (3, 7, 8).

In light of the multicomponent system of granule exocytosis, mechanistic insights have mainly been obtained in studies with isolated proteins, *i.e.* perf and/or granzymes, *in vitro*. For gzmB, hundreds of possible substrates have been considered, but in most instances their biological relevance is unclear (5, 9). Two major apoptotic pathways have been proposed for gzmB, both terminally activating effector caspase-3. gzmB may directly process procaspase-3 (10, 11). Alternatively, gzmB engages the mitochondrial death pathway by converting Bid to tBid (11–16). In turn, tBid oligomerizes Bak and Bax, which permeabilize mitochondria. Factors are released that enhance (*e.g.* cytochrome *c*) and de-repress (*e.g.* SMAC/Diablo) mitochondrial

[4] The abbreviations used are: Tc, cytotoxic T cell; gzmB, granzyme B; perf, perforin; MOMP, mitochondrial outer membrane permeabilization; fmk, cycloheximide; PFA, paraformaldehyde; PS, phosphatidylserine; MEF, mouse embryonic fibroblast; LCMV, lymphocytic choriomeningitis virus; MACS, magnet-activated cell sorting; 7-AAD, 7-amino-actinomycin D.

apoptosome formation (17, 18), controlling caspase-3 activation.

Nevertheless, the factors that initiate and perpetuate the engagement of these pathways *in vivo* have not been fully clarified (9). In this regard, biochemical studies suggest that the pathway(s) engaged may depend on the species of gzmB as well as the source and quality of target cells (19–21). Thus, mouse gzmB seems to mainly process pro-caspase-3 to its active form directly, whereas human gzmB preferentially induces active caspase-3 indirectly by cleaving Bid, which modulates subsequent mitochondrial processes. Adding another dimension, isolated human gzmB has been shown to cleave the anti-apoptotic protein, Mcl-1, thereby releasing the pro-apoptotic BH3-only protein Bim (22). Bim down-regulation by siRNA completely blocks human gzmB-induced apoptosis. Bim is a BH3-only member of the Bcl-2 family, which has been shown to activate Bak and/or Bax directly, independent of other BH3-only proteins like Bid (23–25). The combined studies suggest that caspase-3 and Bid are not the only intracellular targets of gzmB (26).

To closely simulate events *in vivo*, we have delineated apoptotic pathways with mouse *ex vivo* virus-immune Tc cells that selectively kill by a perf/gzmB-dependent mechanism (11, 27). Here, we analyze the role of Bim in gzmB-mediated apoptosis, using spontaneously (3T9) or virus (SV40)-transformed MEF cells and their Bim- or Bak/Bax-deficient variants. We have unexpectedly learned that, in contrast to SV40 MEF cells, apoptosis triggered in 3T9 MEF cells depends upon activation of the mitochondrial death pathway mediated by Bim. These results indicate that the preferred cell death pathway activated by gzmB is not only influenced by the species of the protease but also depends upon the transformation state of the target cell subject to Tc cell attack.

EXPERIMENTAL PROCEDURES

Mouse Strains

Inbred B6 and mouse strains deficient for gzmA (gzmA$^{-/-}$), gzmAxB (gzmAxB$^{-/-}$), and perfxgzmAxgzmB (PAB$^{-/-}$), bred on the B6 background, were maintained at the Agrifood Research and Technology Centre of Aragón, and genotypes were analyzed as described (27). Mice (8–10 weeks old) were studied and were used in accordance with the Federation of Laboratory Animal Science Association guidelines under the supervision and approval of Comite Etico para la Experimentacion Animal (Ethics Committee for Animal Experimentation) from Agrifood Research and Technology Centre of Aragón (number 2011-01).

Cells

Mouse embryonic fibroblasts were cultured in DMEM with 10% FBS at 37 °C, 5% CO$_2$. BakxBax$^{-/-}$ SV40-transformed MEFs were generously provided by Dr. Christoph Borner (Institute of Molecular Medicine and Cell Research, Center for Biochemistry and Molecular Research, Freiburg, Germany) (28) and compared with a MEF WT cell line generated by the same group. Bim$^{-/-}$ 3T9-transformed MEFs and Bim$^{-/-}$ SV40-transformed MEFs were generously provided by Dr. Andeas Strasser (Walter and Eliza Hall Institute of Medical Research, Melbourne, Australia) and Gabriel Gil (Institut Municipal d'Investigació Mèdica, Barcelona, Spain), respectively, and compared with a MEF WT cell line generated by the same group.

BakxBax$^{-/-}$ 3T9-transformed MEFs were generously provided by Dr. Christoph Borner. Caspase-3x7$^{-/-}$ MEF cells were generously provided by Dr. Richard Flavell. In some cases, the caspase-3 inhibitor Ac-DEVD-fmk (Bachem; 100 μM) was added to cell cultures as described (27).

Generation of Ex Vivo Virus-specific CD8$^+$ T Cells

Mice were infected with 10^5 pfu of LCMV strain WE intraperitoneally according to established protocols (29). On day 8 postinfection, CD8$^+$ cells were positively selected from spleen using α-CD8-MicroBeads (Miltenyi Biotec, Germany) with a MACS (Miltenyi Biotec) and resuspended in RPMI 1640 medium and 5% heat-inactivated FBS before use in cytotoxic assays. Purity of selected CD8$^+$ cells was assessed by FACS staining and found to be between 95 and 98% in all cases.

Ex Vivo Cytotoxicity Assay

Target cells were preincubated with the LCMV-immunodominant peptide gp33 (Neosystem Laboratoire) for 1–2 h, and *ex vivo* CD8$^+$ cells were stained with CellTracker Green (Invitrogen). Effector and target cells were incubated at a ratio of 10:1 (effector/target) at 37 °C. Subsequently, different apoptotic parameters were tested in the CellTracker Green negative target population by FACS with a FACSCalibur (Pharmingen) and CellQuest software.

To perform intracellular stainings, CD8$^+$ cells were not pre-stained with CellTracker Green. Instead, after incubation with target cells, they were labeled with α-CD8-APC mAb (Pharmingen), fixed with 4% paraformaldehyde (PFA) in PBS, and used for the different stainings. In this case, the different parameters were tested in the CD8-negative target population as indicated.

For real time cytotoxic assays, a time-lapse imaging system was performed with a Leica AF6000 LX microscope within a temperature- and CO$_2$-controlled chamber. Effector and target cells were incubated at a ratio of 10:1 (effector/target) in the presence of annexin V-FITC and propidium iodide (10 μg/ml) for 3 h with images acquired every 2 min.

Analysis of Pro-apoptotic Processes by Flow Cytometry

Cell Death Induced by ex Vivo Tc Cells in MEF Cells—For cell membrane and mitochondrial membrane perturbations, phosphatidylserine (PS) exposure on plasma membrane and cell membrane integrity were measured by three-color flow cytometry using annexin-V and 7-AAD as described earlier (27). Changes in mitochondrial membrane potential ($\Delta\Psi_m$) was measured by three-color flow cytometry using the fluorescent probe tetramethylrhodamine ethyl ester (25 nM; Molecular Probes).

Caspase-3 Activation—Caspase-3 activation was analyzed by FACS as described (27). Cells were fixed with 4% PFA and incubated with a FITC-labeled mAb against the active form of caspase-3 (clone C92605; Pharmingen) diluted in 0.1% saponin

in PBS. After two washes, cells were resuspended in 1% PFA and analyzed by flow cytometry.

Cytochrome c Release—Cytochrome *c* release was analyzed by flow cytometry as described earlier (30). Briefly, cells were mildly permeabilized with 25 μg/ml digitonin plus 100 mM KCl on ice for 5 min, washed with cold PBS, fixed in 4% PFA, permeabilized with 0.1% saponin, and incubated with the α-cytochrome *c* mAb 6H2.B4 (BD Biosciences) or with mouse IgG isotype followed by α-mouse-Alexa 488 secondary antibody (Invitrogen). Cells were resuspended in 1% PFA and analyzed by flow cytometry.

Analysis of Mcl-1 and Bcl-X_L Degradation—Cells were permeabilized with 0.1% saponin and 5% FBS in PBS and then incubated with the α-Mcl-1 (Abcam) or α-Bcl-X_L (clone 54H6; Cell Signaling) mAb or with rabbit IgG isotype control followed by α-rabbit-Alexa 488 secondary antibody (Invitrogen). Cells were resuspended in 1% PFA, and Mcl-1 degradation was analyzed by FACS.

Clonogenic Assay

MEF cells were pretreated with the LCMV immunodominant peptide gp33 for 1 h prior to incubation with *ex vivo*-derived LCMV-immune Tc cell at 10:1 effector/target cell ratio at 37 °C. After 4 h, cells were trypsinized, and 100 cells were seeded per well in a final volume of 3 ml in a 6-well plate. Cells were then allowed to grow during 7 days at 37 °C. After that time, medium was removed, and cell colonies were counted after fixing and dying them for 20 min with a mixture of glutaraldehyde (6% v/v) and crystal violet (0.5% w/v) at room temperature.

Western Blot

5×10^5 cells were washed in PBS and lysed in a buffer containing 1% Triton X-100 during 15 min on ice. Soluble protein fraction was recovered by centrifugation and separated by SDS-PAGE. The proteins were then transferred to a PVDF membrane and blocked with 5% fat-free milk. The following primary antibodies (dilution) were incubated overnight at 4 °C: α-Bid (1:5000) from R&D Systems; α-Bim (1:1000) from Calbiochem; α-Bcl-2 (1:500) from Abcam; α-Mcl-1 (1:1000) from Santa Cruz Biotechnology; α-Bak (1:1000) from Abcam; α-Bax (1:500), α-XIAP (1:250), α-cytochrome *c* (1:1000), and α-Smac/DIABLO (1:1000) from BD Biosciences; and α-caspase-3 (1:1000) and α-caspase-9 (1:1000) from Cell Signaling. Subsequently, after a washing step and depending on the primary antibody used, blots were incubated during 1 h at room temperature with secondary α-mouse or α-rabbit IgG antibodies conjugated with HRP (Sigma) at a 1:20,000 dilution.

siRNA Transfection

Stealth RNAi™ siRNAs (Life Technologies) were used to knock down Bim and Bid expression in MEF cells. siRNAs were transfected with HiPerfect transfection reagent (Qiagen). The next sequences used were as follows: Bim siRNA, 5′-TCCGCT-TATTTAAATGTCTTA-3′; Bid siRNA, 5′-AUCAGCAUG-GCCUUGUCGUUCUCCA-3′; and control siRNA, 5′-CAC-CCTCAAATGGTTATCTTA-3′.

Drug-induced Cell Death Assay

10^5 cells were cultured with 40 μM sorafenib (Bayer) or 2.0 nM bortezomib (Millennium Pharmaceuticals) for 18 h in DMEM, 10% heat-inactivated FBS. Subsequently, PS exposition was measured by FACS as described above.

Determination of HLA-I Surface Expression by Flow Cytometry

2×10^5 cells were stained for 15 min at 4 °C with anti-H-2K^b-FITC or isotype control (rabbit IgG-FITC) in 100 μl of PBS, 5% FBS. Both antibodies were obtained from BD Biosciences. Cells were washed and analyzed by flow cytometry.

Statistical Analysis

The statistical analysis of the difference between means of independent samples was performed using the unpaired *t* test. The results are given as the confidence interval (*p*) and are considered significant when they are <0.05.

RESULTS AND DISCUSSION

Bim-deficient 3T9 MEF Cells Resist Cell Death Induced by gzmB$^+$ Tc Cells—We have established an *in situ* mouse model to characterize apoptotic processes induced by perf and gzmB using *ex vivo* LCMV-specific Tc cells obtained from mice deficient in gzmA (gzmB$^+$Tc). gzmB$^+$Tc cells kill a variety of targets, including EL4, MC57G, and virus-transformed MEF cells (SV40) in short term assays via perf and gzmB (11, 27, 29). Using this model, we examined the role of Bim during the activation of the mitochondrial cell death pathway in spontaneously (3T9) and virally transformed (SV40) MEF cells. As described previously for SV40 MEF cells (11), gzmB$^+$Tc cells also kill 3T9 MEF cells through a perf and gzmB pathway, without engaging the extrinsic cell death pathway mediated by FasL or tumor necrosis factor-related apoptosis-inducing ligand (TRAIL) (Fig. 1). Indeed, SV40 and 3T9 MEF cells are resistant to both recombinant TRAIL as well as to the cytotoxic anti-Fas antibody Jo-2 (data not shown). The apoptotic phenotype was confirmed by time-lapse fluorescence microscopy (see Fig. 1*C*). WT 3T9 MEF cells labeled with gp33 peptide and incubated with gzmB$^+$Tc showed extensive membrane blebbing and PS translocation (annexin V reactivity) prior to plasma membrane damage (propidium iodide uptake) and nuclear condensation. However, these changes were not observed in control 3T9 MEF cells or in 3T9 MEF cells incubated with gzmB$^+$Tc in the absence of gp33 peptide.

Human gzmB has been shown to induce cell death in Jurkat cells by degradation of Mcl-1 and subsequent release of proapoptotic Bim (22, 26, 31). We therefore asked whether Bim also contributes to gzmB-mediated apoptosis in mice by incubating *ex vivo* mouse gzmB$^+$ Tc cells with either WT or Bim-deficient 3T9 MEF cells (3T9 MEF.Bim$^{-/-}$). Compared with WT cells, PS translocation as well as membrane permeabilization (7-AAD) were completely abolished, and mitochondrial depolarization was significantly reduced in 3T9 MEF.Bim$^{-/-}$ (Fig. 2, *A* and *B*). The results therefore indicate a major role for Bim in the execution of 3T9 cells by *ex vivo* gzmB secreting Tc cells, the most physiological model currently available for the study of cytotoxic cell granule-mediated apoptosis. As
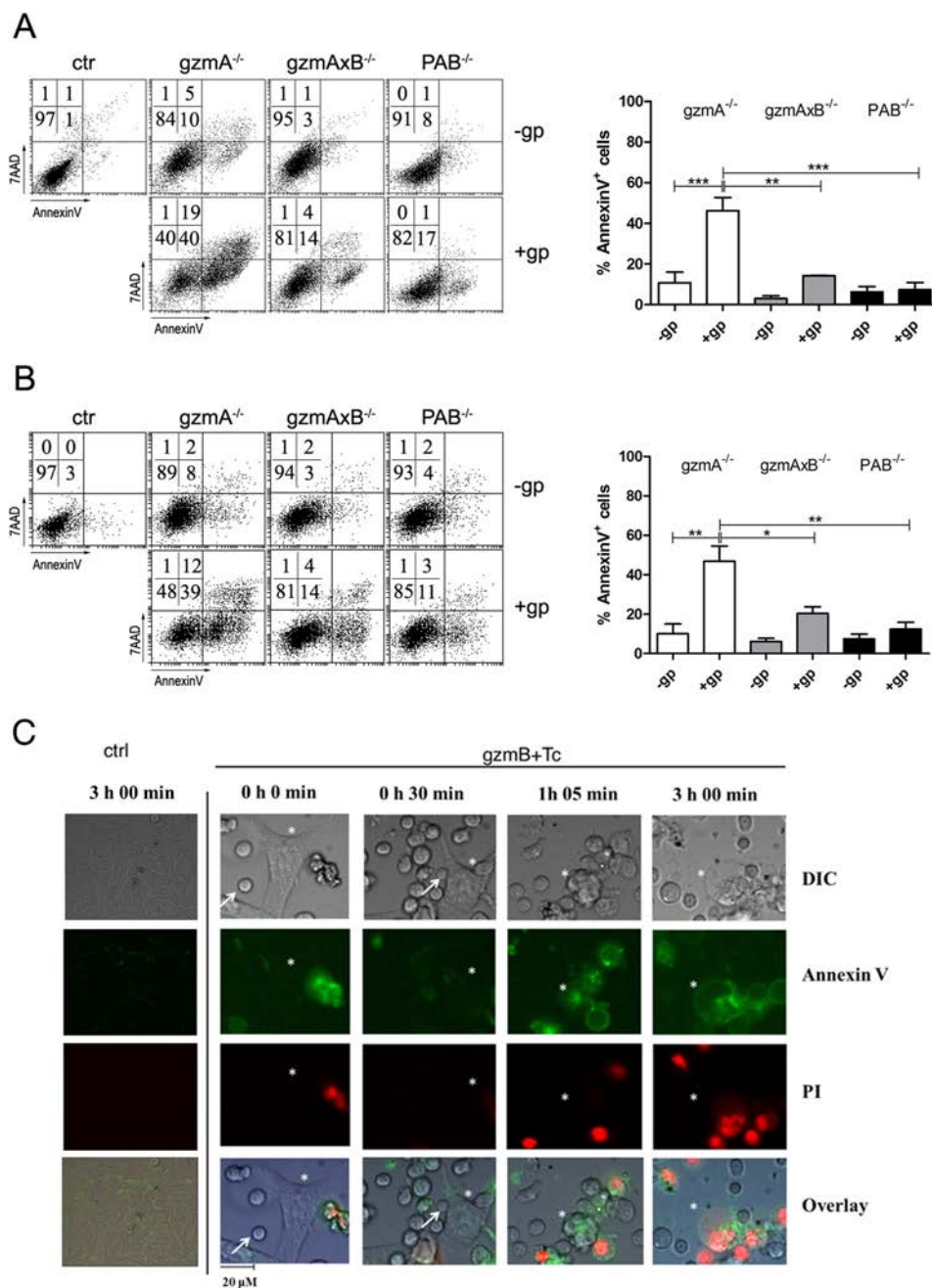
FIGURE 1. **Cell death induced by *ex vivo*-derived LCMV-specific Tc cells from gzmA$^{-/-}$, gzmAxB$^{-/-}$, and perfxgzmAxB$^{-/-}$ (PAB$^{-/-}$) mouse strains.** 3T9 MEF WT (*A*) and SV40 MEFWT (*B*) cells were incubated with *ex vivo* virus immune CD8$^+$ cells from either gzmA$^{-/-}$, gzmAxB$^{-/-}$, and PAB$^{-/-}$ mice in the presence (+*gp*) or absence (−*gp*) of the LCMV peptide gp33 for 3 h. Subsequently, PS exposure on plasma membrane (annexin-V-FITC) and 7-AAD uptake were analyzed by three-color flow cytometry in the cell population negative for CD8 expression as described under "Experimental Procedures." A representative experiment is shown in the *left panels*. *Numbers* correspond to the percentage of cells in each quadrant. Data in the *right panel* are represented as the mean ± S.D. of three independent experiments. *, $p < 0.05$; **, $p < 0.01$; ***, $p < 0.001$. *No symbol* means not significant. *C*, 3T9 MEF WT cells were incubated with *ex vivo* virus immune CD8$^+$ cells from gzmA$^{-/-}$ mice in the presence of the LCMV peptide gp33, annexin V-FITC, and PI for 3 h. Sequential images were taken every 2.5 min as indicated under "Experimental Procedures." *DIC*, differential interference contrast.

expected (32), similar results were obtained with 3T9 MEF cells deficient in the downstream effectors, Bak and Bax (3T9 MEF.BakxBax$^{-/-}$).

Notably, the fact that Bim-deficient 3T9 MEF cells were similarly sensitive to the cytotoxic effect of the protein kinase inhibitor, sorafenib, or the proteasome inhibitor, bortezomib (Fig. 2*C*), indicates that their resistance to gzmB$^+$ Tc cell-mediated apoptosis is not due to a generalized refractory state of the transformed cell line. Supporting

this hypothesis, we show that Bim down-regulation by siRNA in WT 3T9 MEF cells inhibits PS translocation as well as membrane permeabilization induced by (gzmB$^+$Tc cells (Fig. 2*D*)). In the presence of the caspase-3 inhibitor, Ac-DEVD-fmk, PS translocation, membrane permeabilization (Fig. 2*A*), and mitochondrial depolarization mediated by gzmB$^+$ Tc cell (Fig. 2*C*) were reduced in WT 3T9 MEF cells, confirming that induction of these three parameters requires active caspase-3 (11, 27, 33).
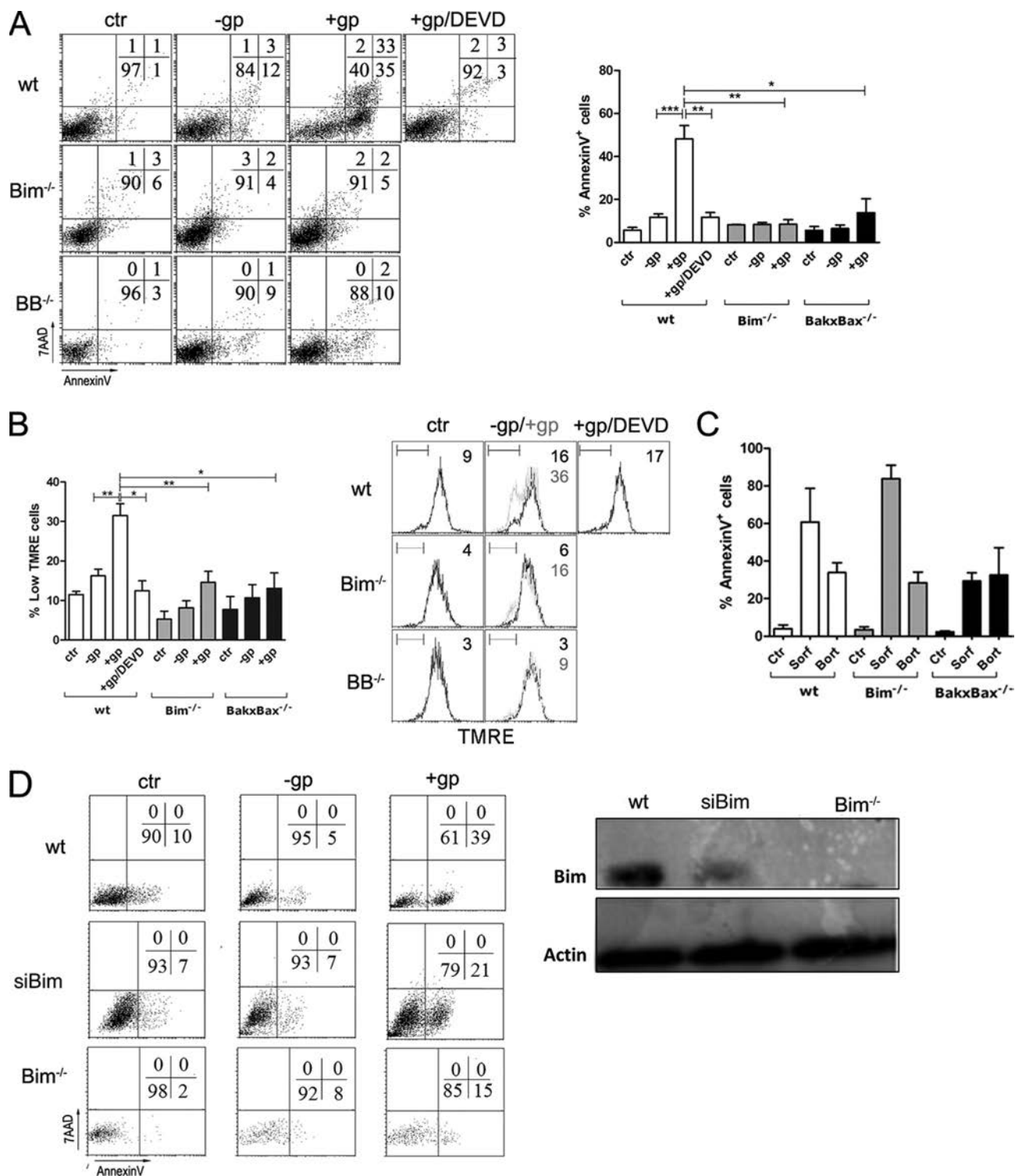
FIGURE 2. **gzmB$^+$ Tc cells induce cell death in 3T9 MEF.WT but neither in 3T9 MEF.Bim$^{-/-}$ nor in 3T9 MEF.BakxBax$^{-/-}$.** MEF.WT, MEF.Bim$^{-/-}$, and MEF.BakxBax$^{-/-}$ cells were incubated with *ex vivo* virus-immune CD8$^+$ cells from gzmA$^{-/-}$ mice, in the presence (+*gp*) or absence (−*gp*) of the LCMV peptide gp33 for 3 h. Subsequently, PS exposure on plasma membrane (annexin-V-FITC) and 7-AAD uptake (*A*) and, in parallel, ΔΨm loss (TMRE, *B*) were analyzed by three-color flow cytometry in the cell population negative for CD8 expression as described under "Experimental Procedures." In some cases MEF cells were also preincubated with the caspase inhibitor Ac-DEVD-fmk 100 μM. *A*, representative experiment is shown in the *left panels*. *Numbers* correspond to the percentage of cells in each quadrant. Data in the *right panel* are represented as the mean ± S.D. of three independent experiments. *B, histograms* show a representative experiment of three independent experiments. *Numbers* correspond to the percentage of cells in regions marked by the *horizontal bar*. Data in the *left panel* are represented as the mean ± S.D. of three independent experiments. *C*, MEF.WT, MEF.Bim$^{-/-}$, and MEF.BakxBax$^{-/-}$ cells were incubated with sorafenib (*Sorf*, 40 mM) and bortezomib (*Bort*, 20 mM) for 18 h. Subsequently, PS exposure on plasma membrane (annexin-V-FITC) was analyzed. Data in this panel are represented as the mean ± S.D. of two independent experiments. *, $p < 0.05$; **, $p < 0.01$; ***, $p < 0.001$. *No symbol* means not significant. *D*, MEF.WT, MEF.Bim$^{-/-}$, or MEF.WT cells treated with siRNA against Bim (*siBim*) were incubated with *ex vivo* virus immune CD8$^+$ cells from gzmA$^{-/-}$ mice, in the presence (+*gp*) or absence (−*gp*) of the LCMV peptide gp33 for 3 h. Subsequently, PS exposure on plasma membrane (annexin-V-FITC) and 7-AAD uptake were analyzed. Bim expression in WT, Bim$^{-/-}$, and siBim-treated cells was analyzed by immunoblot (BimEL isoform). Actin served as loading control.
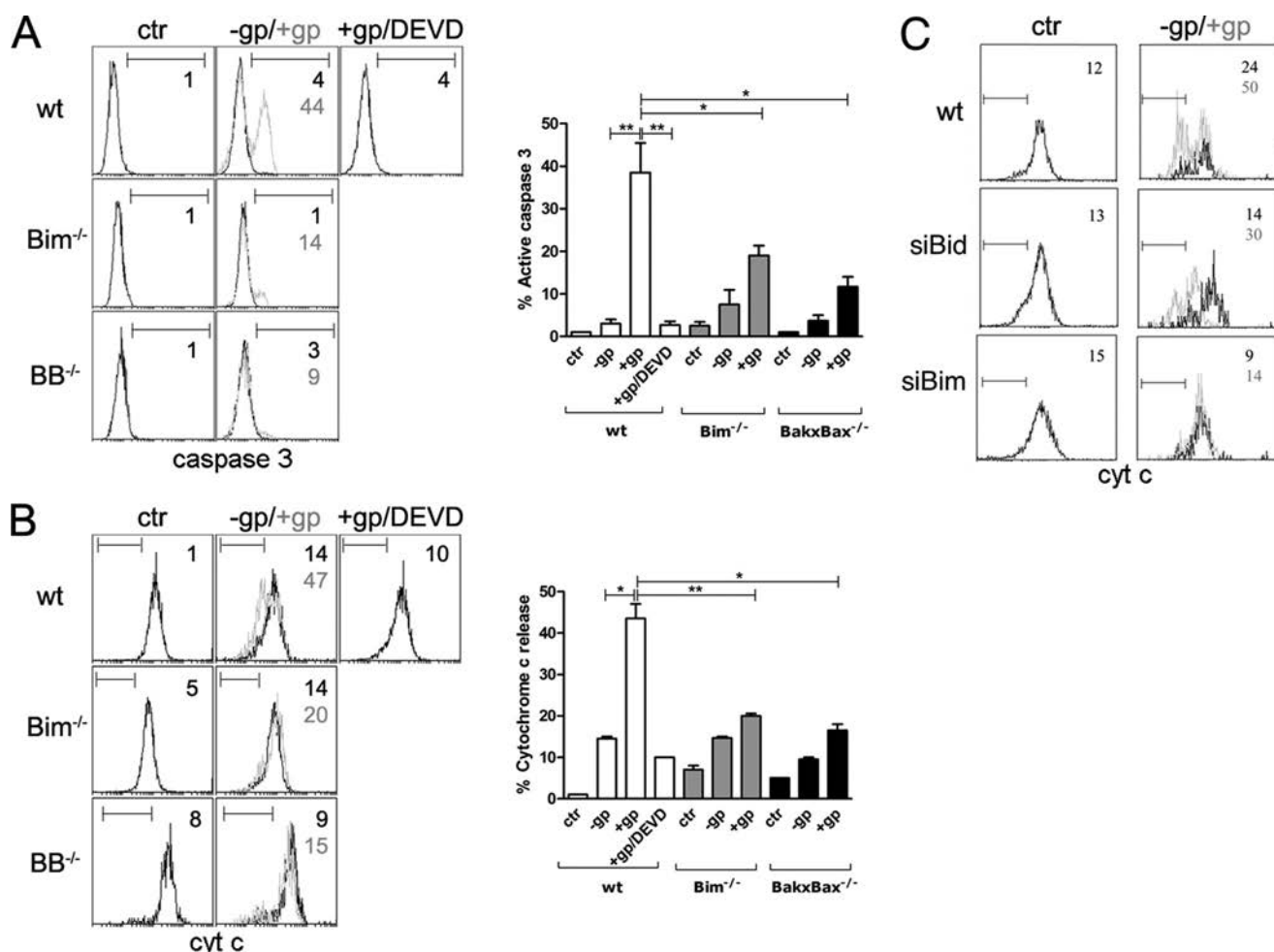
FIGURE 3. **Caspase-3 activation and cytochrome *c* release induced by gzmB$^+$ Tc cell in 3T9 MEF.** MEF.WT, MEF.Bim$^{-/-}$, and MEF.BakxBax$^{-/-}$ cells or MEF.WT cells treated with a siRNA against Bim (*siBim*) or Bid (*siBid*) were incubated with *ex vivo* virus-immune CD8$^+$ cells from gzmA$^{-/-}$ mice, in the presence (+*gp*) or absence (−*gp*) of the LCMV peptide gp33 for 3 h (*A*) or 2 h (*B*). *A*, caspase-3 activation was analyzed by flow cytometry in the target cell population with a mAb against the active form of caspase-3. *Histograms* show a representative experiment of three independent experiments. *Numbers* correspond to the percentage of cells with activated caspase-3, limited by regions marked by the *horizontal bar*. Data in the *right panel* are represented as the mean ± S.D. of three independent experiments. *B,* cytochrome *c* release from mitochondria was analyzed by flow cytometry in the cell population negative for CD8 expression as described under "Experimental Procedures." *Histograms* show a representative experiment of two independent experiments. Data in the *right panel* are represented as the mean ± S.D. of two independent experiments. *, $p < 0.05$; **, $p < 0.01$. *No symbol* means not significant. *C,* MEF.WT cells were treated with a siRNA against Bim (*siBim*) or Bid (*siBid*) and incubated with *ex vivo* virus immune CD8$^+$ cells from gzmA$^{-/-}$ mice, in the presence (+*gp*) or absence (−*gp*) of the LCMV peptide gp33 for 2 h. Cytochrome *c* release from mitochondria was analyzed by flow cytometry in the cell population negative for CD8 expression as described under "Experimental Procedures."

Caspase-3 Activation Induced by gzmB$^+$ Tc Cells Depends on Bim Expression—The demonstration that gzmB$^+$ Tc cell-induced PS translocation and mitochondrial depolarization are suppressed by Ac-DEVD-fmk in WT 3T9 MEF prompted us to analyze the sequence of pro-apoptotic events elicited by gzmB in 3T9 MEF cells. Accordingly, we analyzed caspase-3 activation in 3T9 MEF.Bim$^{-/-}$ cells exposed to gzmB$^+$ Tc cells. The level of active caspase-3 was markedly but not completely reduced in the 3T9 MEF.Bim$^{-/-}$ cells (Fig. 3*A*), suggesting that activation of caspase-3 largely depends on expression of Bim and subsequent induction of mitochondrial processes. This hypothesis was further supported by the data that caspase-3 activation was similarly reduced in 3T9 MEF.BakxBax$^{-/-}$ cells upon incubation with gzmB$^+$ Tc cells (Fig. 3*A*).

Activation of caspase-3 via the mitochondrial pathway has been shown to depend on the release of cytochrome *c* from

Bak/Bax-permeabilized mitochondria and its formation, together with dATP, Apaf-1, and caspase-9, of the apoptosome (34). To confirm that the reduction of caspase-3 activation observed in 3T9 MEF.Bim$^{-/-}$ and BakxBax$^{-/-}$ cells correlated with reduced cytochrome *c* release, this release was measured in target cells incubated with gzmB$^+$ Tc cells (11). Slightly modified from the technique reported by Waterhouse and Trapani (30), this assay determines the level of intramitochondrial cytochrome *c* in target cells exposed to Tc cells. gzmB$^+$ Tc cells readily induced cytochrome *c* release from the mitochondria of 3T9 MEF.WT cells but not in MEF cells, which lacked either Bim or both Bak and Bax (Fig. 3*B*). Furthermore, cytochrome *c* release was completely inhibited by DEVD-fmk suggesting that mitochondrial outer membrane permeabilization (MOMP) requires caspase-3 activation upstream of the mitochondria. Although 3T9 MEF cells express high levels of Bid (Fig. 5), it seems that, in contrast to other cell types, Bid is not able to
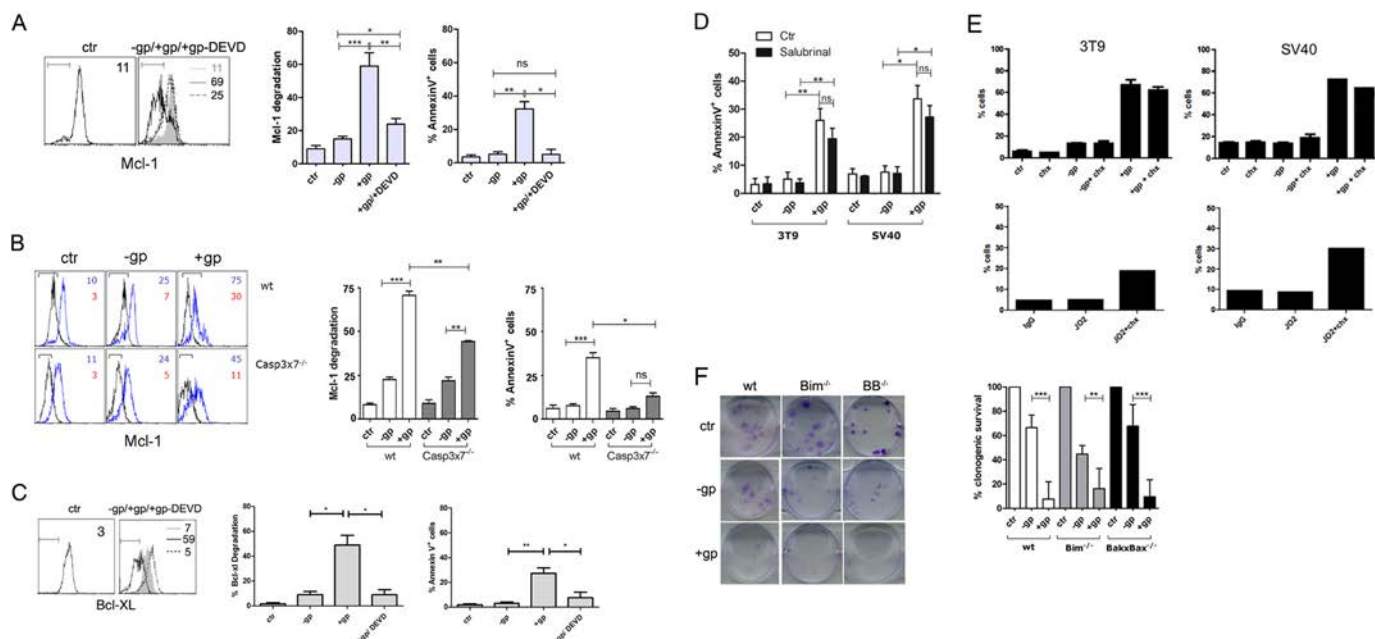
FIGURE 4. **Mcl-1 and Bcl-X$_L$ degradation, transcriptional regulation of Bim and survival assay.** *A–C,* 3T9 or SV40 MEF.WT and MEF.Casp3x7$^{-/-}$ (B) cells were incubated with *ex vivo* virus-immune CD8$^+$ cells from gzmA$^{-/-}$ mice, in the presence (+*gp*) or absence (−*gp*) of the LCMV peptide gp33 for 3 h. Mcl-1 and Bcl-X$_L$ degradation was analyzed by flow cytometry in the target cell population with a mAb against a specific Mcl-1 epitope. *Histograms* show a representative experiment of three independent experiments. *Numbers* correspond to the percentage of cells with Mcl-1 degraded, limited by regions marked by the *horizontal bar*. In the second histogram (*A* and *C*), the *filled histograms* represent cells without gp33 (−*gp*), *black line* represents cells plus gp33 (+*gp*). and *broken line* represents cells with gp33 plus DEVD (+*gp-DEVD*). *B, black* and *blue* histograms correspond to the isotype antibody control and Mcl-1 specific mAb, respectively. *Numbers* in *gray* corresponds to the % of annexin V$^+$ cells. Data in the *right panel* are represented as the mean ± S.D. of three independent experiments. *D* and *E,* gp33-pulsed 3T9 MEF.WT and SV40 MEF.WT cells were incubated with *ex vivo* virus-immune CD8$^+$ cells from gzmA$^{-/-}$ mice in the presence of salubrinal, 10 μM (*D*), or cycloheximide (*chx*) (*E*) for 2 h. Subsequently, PS exposure on plasma membrane (annexin-V-FITC) was analyzed. Data in this panel are represented as the mean ± S.D. of two independent experiments. *, $p < 0,05$; **, $p < 0,01$; *ns*, not significant. *F,* for survival assay, MEF.WT, MEF.Bim$^{-/-}$, and MEF.BakxBax$^{-/-}$ cells were incubated with *ex vivo* virus-immune CD8$^+$ cells from gzmA$^{-/-}$ mice, in the presence (+*gp*) or absence (−*gp*) of the LCMV peptide gp33. 3 h after incubation, cells were washed, trypsinized, and counted. 100 cells per well were seeded in 6-well plates and incubated in fresh medium for 7 days. After incubation, cells were stained with crystal violet, and colonies were counted. Survival was calculated as percentage of colonies relative to the colonies in the controls. Values were represented as the mean ± S.D. of four independent experiments. *, $p < 0,05$; **, $p < 0,01$; ***, $p < 0,001$. *No symbol* means not significant.

initiate cytochrome *c* release in 3T9 MEF cells. This hypothesis is confirmed in Fig. 3*C* where siRNA against Bid only partially reduces cytochrome *c* release, meanwhile siRNA against Bim completely blocked release.

These results suggest that gzmB directly activates caspase-3 (Fig. 3*A*) to initiate MOMP and the release of cytochrome *c*. Because this process also depends on Bim and Bak and Bax (Fig. 3*B*), altogether our data suggest that activation of the mitochondrial pathway mediated by Bim occurs through caspase-3 when intact Tc cells are examined.

gzmB$^+$ Tc Cells Initiate Degradation of the Anti-apoptotic Protein, Mcl-1, in 3T9 MEF Cells—Isolated human gzmB has been shown to directly cleave Mcl-1 in human target cells blocking its ability to inhibit the pro-apoptotic activity of Bim (22, 26). However, our data (Fig. 3) suggest that this process could be mediated by caspase-3 in the mouse system. We therefore determined whether Mcl-1 is similarly degraded in mouse target cells incubated with mouse gzmB$^+$ Tc cells and whether caspases-3 and -7 are participants in this process. Because Mcl-1 is also highly expressed in *ex vivo* Tc cells, the detection of processed target cell-associated Mcl-1 by immunoblot is problematic. To avoid this technical pitfall, a protocol was established to measure Mcl-1 degradation by flow cytometry. A mAb against a peptide that contained the site cleaved by human gzmB and caspase-3 (Asp-127) was used to monitor the level of

intact Mcl-1. Conserved in both human and mouse (26), cleavage of this site is predicted to reduce the binding of the detecting mAb. A similar approach has been successfully employed to analyze the cleavage of other gzm substrates by Tc cells (27).

Upon incubation with gzmB$^+$ Tc cells, the expression of Mcl-1 in nonpulsed 3T9 MEF cells (−gp) is rather homogeneous (Fig. 4*A*). In contrast, Mcl-1 expression was lost in most gp33-pulsed 3T9 MEF cells (70%) under similar conditions. Loss of Mcl-1 preceded signs of cell death indicating that its degradation designated an early proteolytic event during gzmB-induced cell death and was not due to protein loss in dying cells. Ac-DEVD-fmk treatment of 3T9 MEF.WT cells significantly reduced the proteolysis of Mcl-1 degradation suggesting that caspase-3 is mainly responsible. Indeed, a similar result was observed in SV40 MEF Casp3x7$^{-/-}$ MEF cells (Fig. 4*B*).

Other anti-apoptotic proteins like Bcl-X$_L$ have also been shown to bind Bim preventing its pro-apoptotic activity. Using an approach similar to Mcl-1, we found that gzmB$^+$Tc also degraded Bcl-X$_L$ (Fig. 4*C*) among WT 3T9 MEF cells in a caspase-dependent manner, suggesting that Bim activation could be mediated by degradation of both Bcl-X$_L$ and Mcl-1. Bcl-2 degradation was not analyzed by FACS because its expression in MEF cells is almost undetectable (data not shown).
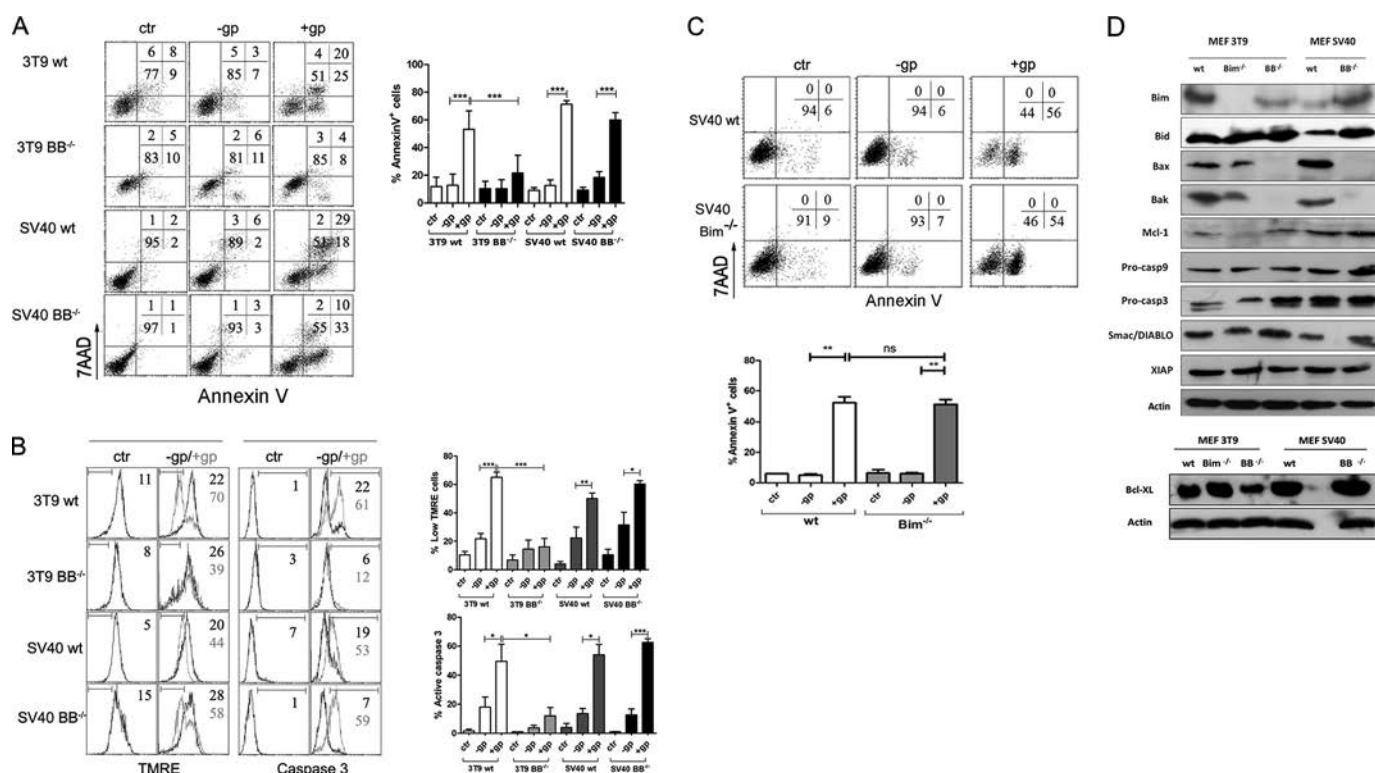
FIGURE 5. **Implication of mitochondrial apoptotic pathway in cell death induced by gzmB$^+$ Tc in MEF 3T9 and MEF SV40.** 3T9 MEF.WT, 3T9 MEF.BakxBax$^{-/-}$, SV40 MEF.WT, and SV40 MEF.BakxBax$^{-/-}$ cells were incubated with *ex vivo* virus-immune CD8$^+$ cells from gzmA$^{-/-}$ mice in the presence (+*gp*) or absence (−*gp*) of the LCMV peptide gp33 for 3 h. Subsequently, PS exposure on plasma membrane (annexin-V-FITC) and 7-AAD uptake (*A*) and, in parallel, $\Delta\Psi$m loss (TMRE) and caspase-3 activation (*B*) were analyzed by three-color flow cytometry in the cell population negative for CD8 expression. *A*, representative experiment is shown in the *left panels*. *Numbers* correspond to the percentage of cells in each quadrant. Data in the *right panel* are represented as the mean ± S.D. of six independent experiments. *B*, histograms show a representative experiment of three independent experiments. *Numbers* correspond to the percentage of cells in regions marked by the *horizontal bar*. *C*, SV40 MEF.WT and SV40 MEF.Bim$^{-/-}$ cells were incubated with *ex vivo* virus-immune CD8$^+$ cells from gzmA$^{-/-}$ mice, in the presence (+*gp*) or absence (−*gp*) of the LCMV peptide gp33 for 3 h. Subsequently, PS exposure on plasma membrane (annexin-V-FITC) and 7-AAD uptake was analyzed by three-color flow cytometry in the cell population negative for CD8 expression. A representative experiment is shown in the *left panels*. *Numbers* correspond to the percentage of cells in each quadrant. Data in the *right panel* are represented as the mean ± S.D. of two independent experiments. *, $p < 0.05$; **, $p < 0.01$; ***, $p < 0.001$. *No symbol* means not significant. Data in the *right panels* are represented as the mean ± S.D. of three independent experiments. *D*, lysates of MEF 3T9 WT, MEF 3T9 Bim$^{-/-}$, MEF 3T9 BakxBax$^{-/-}$, MEF SV40 WT, and MEF SV40 BakxBax$^{-/-}$ cells were prepared and Bim (BimEL isoform), Bid, Bak, Bax, Bcl-X$_L$, Mcl-1, XIAP, Smac/DIABLO, caspase-3, and caspase-9 expression were analyzed by Western blot as described under "Experimental Procedures." Actin was used as loading control.

The endoplasmic reticulum stress inhibitor, salubrinal (35), which transcriptionally regulates Bim, did not alter gzmB$^+$ Tc-induced apoptosis in 3T9 cells (Fig. 4*D*). Bim expression is therefore not likely to be regulated by endoplasmic reticulum stress pathways (36), a notion consistent with the observation that gzmB Tc-mediated cell death is an extremely rapid phenomenon (37). Because the inhibitor of protein synthesis, cycloheximide, was inactive (Fig. 4*E*), other pathways of transcriptional regulation of Bim were not examined. As control, cycloheximide sensitized MEF cells to apoptosis induced by the cytotoxic anti-Fas antibody JO2.

To efficiently induce cell death, the participation of Bim and the subsequent induction of the mitochondrial pathway appear essential. However, the exact mechanism by which gzmB$^+$ Tc initiates this process is not completely clear. Our findings suggest that gzmB cleaves a small amount of caspase-3 which, in turn, cleaves Mcl-1 and inhibits its ability to block pro-apoptotic Bim. Subsequently, Bim would activate the mitochondrial apoptotic pathway heightening caspase-3 activation. This amplification loop therefore seems necessary to maximize PS translocation and other signs of apoptosis. Notably, a small quantity of Mcl-1 is cleaved in the absence of caspase-3 and

caspase-7 (Fig. 3), but this amount is not sufficient to induce MOMP and activation of the mitochondrial cell death pathway because inhibition of caspases entirely blocks cytochrome *c* release (Fig. 3*B*). This mechanism is supported by previous findings showing that cleavage by caspases or granzyme B after Asp-127 and Asp-157 residues generate Mcl-1 fragments that bind Bim (26, 38). However, for unclear reasons, these fragments do not interfere with the pro-apoptotic activity of Bim.

Cleavage of Mcl-1 may not be sufficient to activate pro-apoptotic Bim because other anti-apoptotic proteins, especially Bcl-X$_L$, have been shown to block Bim (39, 40). We also show that Bcl-X$_L$ is degraded during cell death induced by gzmB$^+$Tc (Fig. 4*C*), thus both Mcl-1 and Bcl-X$_L$ degradation may be necessary for optimal participation of Bim during apoptosis induced by gzmB-associated Tc cells.

Absence of Bim Does Not Protect Cells from gzmB$^+$Tc in a Clonogenic Survival Assay—To determine whether target cells lacking Bim or Bak/Bax unequivocally resist gzmB$^+$ Tc cells, we examined the susceptibility with the clonogenic assay. MEF cells deficient in either Bim or Bak and Bax similarly do not have a survival advantage that exceeded WT cells (Fig. 4*F*). Therefore, loss of Bim does not confer an absolute resistance to perf

and gzmB delivered by intact Tc. These data indicate that Bim, Bak, and Bax contribute to the induction of apoptotic processes, as defined by a number of *in vitro* markers, but in their absence other gzmB-mediated pathways are likely operative to kill MEF cells as defined by the clonogenic assay. These data support previous findings showing that the simultaneous blockade of mitochondrial and caspase-3 pathways does not result in long term survival of target cells upon their exposure to gzmB$^+$ Tc (11).

Mitochondrial Apoptotic Pathway Is Involved in gzmB$^+$ Tc Cell-mediated Apoptosis of 3T9 but Not SV40 MEF Cells—Our results indicate that gzmB$^+$Tc cell-induced apoptosis of 3T9 MEF cells is dependent on the participation of Bim, Bak, and Bax. These results contradict previous data showing that both isolated mouse gzmB (16) and mouse gzmB$^+$Tc cells (11) induce apoptosis and cell death of Bak/Bax-deficient SV40 MEF targets.

To analyze whether the molecular mechanism of gzmB-mediated apoptosis is influenced by the type of cell transformation in MEF cells (3T9 *versus* SV40), we compared the potential of gzmB$^+$Tc cells to induce cell death in 3T9 or SV40 MEF cells deficient in Bak and Bax. In contrast to 3T9 MEF.BakxBax$^{-/-}$ cells, SV40 MEF.BakxBax$^{-/-}$ cells as well as both WT MEF cell lines were equally susceptible to gzmB$^+$Tc-induced apoptosis as determined by PS translocation (Fig. 5*A*), membrane permeabilization (Fig. 5*A*), mitochondrial depolarization (Fig. 5*B*), and caspase-3 activation (Fig. 5*B*). Therefore, in this model, the apoptotic processes activated by perf and gzmB are not dictated only by the origin of target cells, but intriguingly by the type of transformation of individual cell lines. Confirming this hypothesis we show, in contrast to 3T9 MEF.Bim$^{-/-}$ cells (see Fig. 1), SV40 MEF.Bim$^{-/-}$ cells are equally susceptible to gzmB$^+$Tc as WT SV40 MEF cells (Fig. 5*C*).

The 3T9- and SV40-associated mutational events that lead to cellular immortalization likely differ, thereby influencing the susceptibility of these targets cells to gzmB$^+$ Tc cell-facilitated apoptotic events. We have measured the expression of several proteins that are involved in gzmB-induced apoptosis, including caspase-9 and -3, Bim, Bid, Bak, Bax, Bcl-2, Bcl-X$_L$, Mcl-1, SMAC/Diablo, and XIAP (Fig. 5*D*). Bcl-2 was not detected in MEF cells (data not shown). The finding that all tested proteins were similarly expressed in both transformed cell lines suggests that more subtle alterations contribute to the relative susceptibility of 3T9 and SV40 cells to gzmB$^+$Tc cell-mediated cytolysis. Thus, a more detailed investigation of proteins mutated in these two cell types is required to further our understanding of the inter-relationship between immortalization, oncogenic transformation, and susceptibility to perf-gzmB-mediated apoptosis.

Our results indicate that gzmB$^+$Tc cells inhibit the clonogenic expansion of both 3T9 (Fig. 4) and SV40 MEF.BakxBax$^{-/-}$ (data not shown) (11) cells, although the apoptotic markers tested are only expressed in SV40 transformed cells. *A priori*, two possible explanations may account for these findings. The cells are not killed by gzmB$^+$ Tc cells but are unable to proliferate. Alternatively, the 3T9 cells are dying without displaying traditional apoptotic markers.

Based on our findings, it is tempting to speculate that mutations, which overcome cell senescence and lead instead to
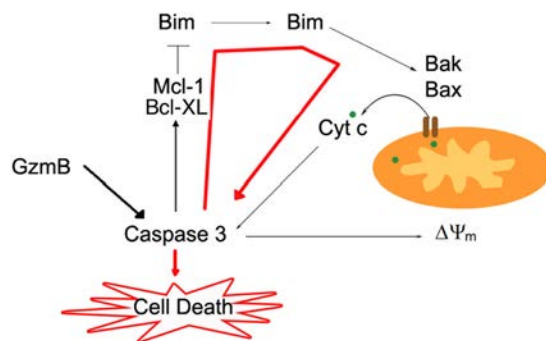

FIGURE 6. Role of Bim during gzmB-induced apoptosis in 3T9 MEF cells. gzmB cleaves a small amount of Mcl-1 and Bcl-X$_L$, which enhances the pro-apoptotic activity of Bim and activates the mitochondrial apoptotic pathway leading to caspase-3 activation. Active caspase-3 would then increase Mcl-1 and Bcl-X$_L$ degradation, Bim release, and heightened caspase-3 activation, an amplification loop that would be required to maximize PS translocation and apoptosis.

immortalization, contribute to the escape of tumor variants that resist gzmB-induced apoptosis (41). Because of the critical importance of perf and gzmB during Tc and natural killer cell-mediated responses, therapeutic endeavors should focus on profiling apoptotic and anti-apoptotic proteins in malignant cells from patients to optimize cancer immunotherapy. The study of a greater number of characterized target cells will be required to support this hypothesis. However, our data unequivocally show that Bim participates in the molecular mechanism of apoptosis induced by perf and gzmB of mouse Tc cells (summarized in Fig. 6), adding another physiologically validated player to the pleiotropic intracellular mechanism of gzmB-induced apoptosis.

REFERENCES

1. Trapani, J. A., and Smyth, M. J. (2002) Functional significance of the perforin/granzyme cell death pathway. *Nat. Rev. Immunol.* **2,** 735–747
2. Ashton-Rickardt, P. G. (2005) The granule pathway of programmed cell death. *Crit. Rev. Immunol.* **25,** 161–182
3. Pardo, J., Aguilo, J. I., Anel, A., Martin, P., Joeckel, L., Borner, C., Wallich, R., Müllbacher, A., Froelich, C. J., and Simon, M. M. (2009) The biology of cytotoxic cell granule exocytosis pathway: granzymes have evolved to induce cell death and inflammation. *Microbes Infect.* **11,** 452–459
4. Lord, S. J., Rajotte, R. V., Korbutt, G. S., and Bleackley, R. C. (2003) Granzyme B: a natural born killer. *Immunol. Rev.* **193,** 31–38
5. Afonina, I. S., Cullen, S. P., and Martin, S. J. (2010) Cytotoxic and non-cytotoxic roles of the CTL/NK protease granzyme B. *Immunol. Rev.* **235,** 105–116
6. Trapani, J. A., and Sutton, V. R. (2003) Granzyme B: pro-apoptotic, antiviral and antitumor functions. *Curr. Opin. Immunol.* **15,** 533–543
7. Trapani, J. A., and Bird, P. I. (2008) A renaissance in understanding the multiple and diverse functions of granzymes? *Immunity* **29,** 665–667
8. Lieberman, J. (2010) Granzyme A activates another way to die. *Immunol. Rev.* **235,** 93–104
9. Hoves, S., Trapani, J. A., and Voskoboinik, I. (2010) The battlefield of perforin/granzyme cell death pathways. *J. Leukocyte Biol.* **87,** 237–243
10. Darmon, A. J., Nicholson, D. W., and Bleackley, R. C. (1995) Activation of the apoptotic protease CPP32 by cytotoxic T-cell-derived granzyme B. *Nature* **377,** 446–448

11. Pardo, J., Wallich, R., Martin, P., Urban, C., Rongvaux, A., Flavell, R. A., Müllbacher, A., Borner, C., and Simon, M. M. (2008) Granzyme B-induced cell death exerted by *ex vivo* CTL: discriminating requirements for cell death and some of its signs. *Cell Death Differ.* **15,** 567–579

12. Alimonti, J. B., Shi, L., Baijal, P. K., and Greenberg, A. H. (2001) Granzyme B induces BID-mediated cytochrome c release and mitochondrial permeability transition. *J. Biol. Chem.* **276,** 6974–6982

13. Barry, M., Heibein, J. A., Pinkoski, M. J., Lee, S. F., Moyer, R. W., Green, D. R., and Bleackley, R. C. (2000) Granzyme B short-circuits the need for caspase 8 activity during granule-mediated cytotoxic T-lymphocyte killing by directly cleaving Bid. *Mol. Cell. Biol.* **20,** 3781–3794

14. Pinkoski, M. J., Waterhouse, N. J., Heibein, J. A., Wolf, B. B., Kuwana, T., Goldstein, J. C., Newmeyer, D. D., Bleackley, R. C., and Green, D. R. (2001) Granzyme B-mediated apoptosis proceeds predominantly through a Bcl-2-inhibitable mitochondrial pathway. *J. Biol. Chem.* **276,** 12060–12067

15. Sutton, V. R., Davis, J. E., Cancilla, M., Johnstone, R. W., Ruefli, A. A., Sedelies, K., Browne, K. A., and Trapani, J. A. (2000) Initiation of apoptosis by granzyme B requires direct cleavage of bid, but not direct granzyme B-mediated caspase activation. *J. Exp. Med.* **192,** 1403–1414

16. Thomas, D. A., Scorrano, L., Putcha, G. V., Korsmeyer, S. J., and Ley, T. J. (2001) Granzyme B can cause mitochondrial depolarization and cell death in the absence of BID, BAX, and BAK. *Proc. Natl. Acad. Sci. U.S.A.* **98,** 14985–14990

17. Goping, I. S., Barry, M., Liston, P., Sawchuk, T., Constantinescu, G., Michalak, K. M., Shostak, I., Roberts, D. L., Hunter, A. M., Korneluk, R., and Bleackley, R. C. (2003) Granzyme B-induced apoptosis requires both direct caspase activation and relief of caspase inhibition. *Immunity* **18,** 355–365

18. Sutton, V. R., Wowk, M. E., Cancilla, M., and Trapani, J. A. (2003) Caspase activation by granzyme B is indirect, and caspase autoprocessing requires the release of proapoptotic mitochondrial factors. *Immunity* **18,** 319–329

19. Casciola-Rosen, L., Garcia-Calvo, M., Bull, H. G., Becker, J. W., Hines, T., Thornberry, N. A., and Rosen, A. (2007) Mouse and human granzyme B have distinct tetrapeptide specificities and abilities to recruit the bid pathway. *J. Biol. Chem.* **282,** 4545–4552

20. Cullen, S. P., Adrain, C., Lüthi, A. U., Duriez, P. J., and Martin, S. J. (2007) Human and murine granzyme B exhibit divergent substrate preferences. *J. Cell Biol.* **176,** 435–444

21. Kaiserman, D., Bird, C. H., Sun, J., Matthews, A., Ung, K., Whisstock, J. C., Thompson, P. E., Trapani, J. A., and Bird, P. I. (2006) The major human and mouse granzymes are structurally and functionally divergent. *J. Cell Biol.* **175,** 619–630

22. Han, J., Goldstein, L. A., Gastman, B. R., Froelich, C. J., Yin, X. M., and Rabinowich, H. (2004) Degradation of Mcl-1 by granzyme B: implications for Bim-mediated mitochondrial apoptotic events. *J. Biol. Chem.* **279,** 22020–22029

23. Sarosiek, K. A., Chi, X., Bachman, J. A., Sims, J. J., Montero, J., Patel, L., Flanagan, A., Andrews, D. W., Sorger, P., and Letai, A. (2013) BID preferentially activates BAK while BIM preferentially activates BAX, affecting chemotherapy response. *Mol. Cell* **51,** 751–765

24. Kim, H., Rafiuddin-Shah, M., Tu, H. C., Jeffers, J. R., Zambetti, G. P., Hsieh, J. J., and Cheng, E. H. (2006) Hierarchical regulation of mitochondrion-dependent apoptosis by BCL-2 subfamilies. *Nat. Cell Biol.* **8,** 1348–1358

25. Hutcheson, J., Scatizzi, J. C., Bickel, E., Brown, N. J., Bouillet, P., Strasser, A., and Perlman, H. (2005) Combined loss of proapoptotic genes Bak or Bax with Bim synergizes to cause defects in hematopoiesis and in thymo-cyte apoptosis. *J. Exp. Med.* **201,** 1949–1960

26. Han, J., Goldstein, L. A., Gastman, B. R., Rabinovitz, A., and Rabinowich, H. (2005) Disruption of Mcl-1·Bim complex in granzyme B-mediated mitochondrial apoptosis. *J. Biol. Chem.* **280,** 16383–16392

27. Pardo, J., Bosque, A., Brehm, R., Wallich, R., Naval, J., Müllbacher, A., Anel, A., and Simon, M. M. (2004) Apoptotic pathways are selectively activated by granzyme A and/or granzyme B in CTL-mediated target cell lysis. *J. Cell Biol.* **167,** 457–468

28. Wei, M. C., Zong, W. X., Cheng, E. H., Lindsten, T., Panoutsakopoulou, V., Ross, A. J., Roth, K. A., MacGregor, G. R., Thompson, C. B., and Korsmeyer, S. J. (2001) Proapoptotic BAX and BAK: a requisite gateway to mitochondrial dysfunction and death. *Science* **292,** 727–730

29. Pardo, J., Balkow, S., Anel, A., and Simon, M. M. (2002) The differential contribution of granzyme A and granzyme B in cytotoxic T lymphocyte-mediated apoptosis is determined by the quality of target cells. *Eur. J. Immunol.* **32,** 1980–1985

30. Waterhouse, N. J., and Trapani, J. A. (2003) A new quantitative assay for cytochrome c release in apoptotic cells. *Cell Death Differ.* **10,** 853–855

31. Joeckel, L. T., Wallich, R., Martin, P., Sanchez-Martinez, D., Weber, F. C., Martin, S. F., Borner, C., Pardo, J., Froelich, C., and Simon, M. M. (2011) Mouse granzyme K has pro-inflammatory potential. *Cell Death Differ.* **18,** 1112–1119

32. Huang, D. C., and Strasser, A. (2000) BH3-Only proteins-essential initiators of apoptotic cell death. *Cell* **103,** 839–842

33. Bleackley, R. C. (2005) A molecular view of cytotoxic T lymphocyte induced killing. *Biochem. Cell Biol.* **83,** 747–751

34. Li, P., Nijhawan, D., Budihardjo, I., Srinivasula, S. M., Ahmad, M., Alnemri, E. S., and Wang, X. (1997) Cytochrome c and dATP-dependent formation of Apaf-1/caspase-9 complex initiates an apoptotic protease cascade. *Cell* **91,** 479–489

35. Boyce, M., Bryant, K. F., Jousse, C., Long, K., Harding, H. P., Scheuner, D., Kaufman, R. J., Ma, D., Coen, D. M., Ron, D., and Yuan, J. (2005) A selective inhibitor of eIF2α dephosphorylation protects cells from ER stress. *Science* **307,** 935–939

36. Puthalakath, H., O'Reilly, L. A., Gunn, P., Lee, L., Kelly, P. N., Huntington, N. D., Hughes, P. D., Michalak, E. M., McKimm-Breschkin, J., Motoyama, N., Gotoh, T., Akira, S., Bouillet, P., and Strasser, A. (2007) ER stress triggers apoptosis by activating BH3-only protein Bim. *Cell* **129,** 1337–1349

37. Metkar, S. S., Wang, B., Catalan, E., Anderluh, G., Gilbert, R. J., Pardo, J., and Froelich, C. J. (2011) Perforin rapidly induces plasma membrane phospholipid flip-flop. *PLoS One* **6,** e24286

38. Herrant, M., Jacquel, A., Marchetti, S., Belhacène, N., Colosetti, P., Luciano, F., and Auberger, P. (2004) Cleavage of Mcl-1 by caspases impaired its ability to counteract Bim-induced apoptosis. *Oncogene* **23,** 7863–7873

39. Zhu, Y., Swanson, B. J., Wang, M., Hildeman, D. A., Schaefer, B. C., Liu, X., Suzuki, H., Mihara, K., Kappler, J., and Marrack, P. (2004) Constitutive association of the proapoptotic protein Bim with Bcl-2-related proteins on mitochondria in T cells. *Proc. Natl. Acad. Sci. U.S.A.* **101,** 7681–7686

40. Vela, L., Gonzalo, O., Naval, J., and Marzo, I. (2013) Direct interaction of Bax and Bak proteins with Bcl-2 homology domain 3 (BH3-only proteins in living cells revealed by fluorescence complementation. *J. Biol. Chem.* **288,** 4935–4946

41. Vesely, M. D., Kershaw, M. H., Schreiber, R. D., and Smyth, M. J. (2011) Natural innate and adaptive immunity to cancer. *Annu. Rev. Immunol.* **29,** 235–271